10.1098/rsta.2004.1482

THE ROYAL SOCIETY

Atmosphere–ocean dynamics in the Western Indian Ocean recorded in corals

By J. Zinke[1], M. Pfeiffer[2], O. Timm[2], W.-C. Dullo[2] and G. R. Davies[1]

[1] *Vrije Universiteit Amsterdam, De Boelelaan 1085, 1081 HV Amsterdam, The Netherlands* (zinj@geo.vu.nl)
[2] *Leibniz Institut für Meereswissenschaften, IFM-GEOMAR, Department of Ocean Circulation and Climate, Wischhofstrasse 1-3, 24148 Kiel, Germany* (mpfeiffer@ifm-geomar.de)

We present a set of *Porites* coral oxygen isotope records from the tropical and subtropical Western Indian Ocean covering the past 120–336 years. All records were thoroughly validated for proxy response to regional climate factors and their relation to large-scale climate modes. The records show markedly different imprints of regional climate factors. At the same time, all coral records show clear teleconnections between the Western Indian Ocean and the El Niño–Southern Oscillation (ENSO). The multi-proxy site analysis enables the detection of the covariance structure between individual records and climate modes such as ENSO. This method unravels shifts in ENSO teleconnectivity of the Western and Central Indian Ocean on multi-decadal time-scales (after 1976). The Seychelles record shows a stationary correlation with ENSO, Chagos corals show evidence for non-stationary δ^{18}O/ENSO relationships and the Southwestern Indian Ocean corals show a strong relationship with ENSO when the forcing is strong (1880–1920, 1970 to present).

Our results indicate that the coral δ^{18}O, in combination with other proxies, can be used to monitor temporal and spatial variations in the sea-surface temperature and the fresh water balance within the Indian Ocean on interannual to interdecadal time-scales.

Keywords: oxygen isotopes; Sr/Ca ratios; El Niño–Southern Oscillation (ENSO); monsoon

1. Introduction

Geochemical parameters in skeletons of massive corals have been used to infer past changes in climate on interannual to multidecadal time-scales, e.g. sea-surface temperature (SST), sea-surface salinity (SSS), upwelling, river run-off and oceanic advection (Cole *et al*. 1993, 2000; Druffel & Griffin 1993; Dunbar *et al*. 1994; McCulloch *et al*. 1994; Charles *et al*. 1997, 2003; Gagan *et al*. 1998; Quinn *et al*. 1998; Kuhnert *et al*. 2000; Le Bec *et al*. 2000; Linsley *et al*. 2000; Juillet-Leclerc & Schmidt

One contribution of 24 to a Discussion Meeting 'Atmosphere–ocean–ecology dynamics in the Western Indian Ocean'.

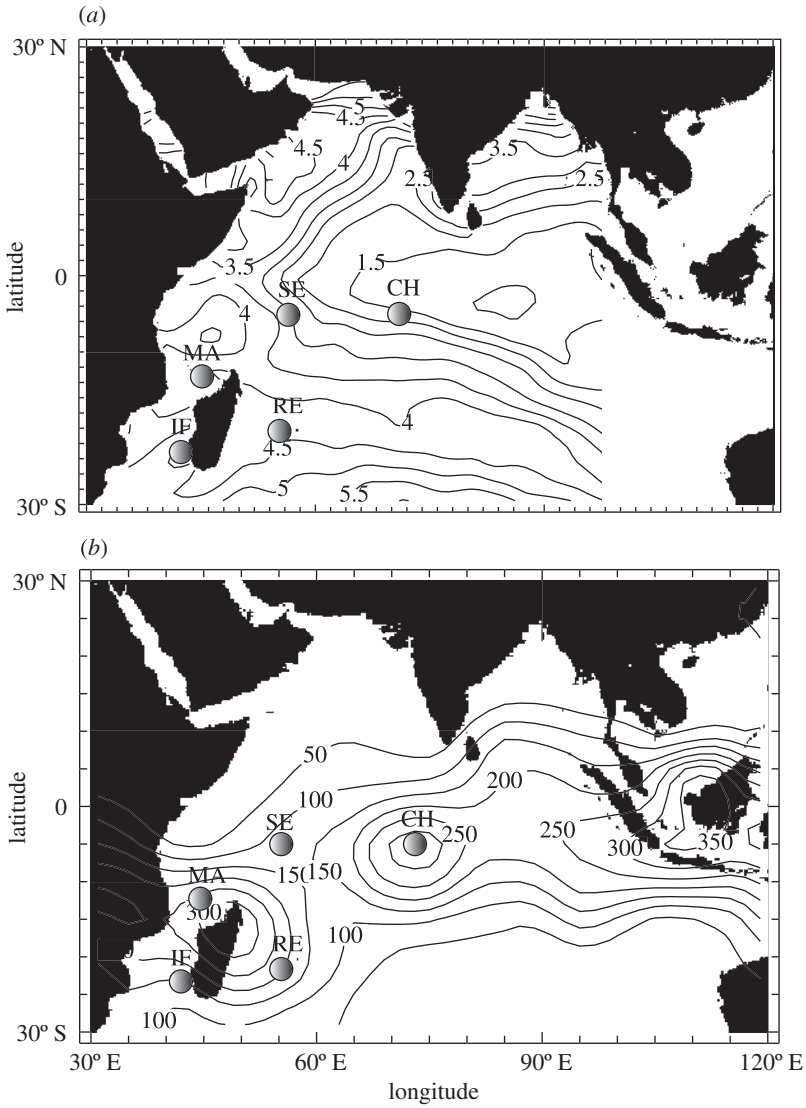

Figure 1. Map of coral core locations superimposed on (*a*) annual SST range averaged between 1981 and 2003 (from Reynolds *et al*. 2002) and (*b*) precipitation climatology (mm per month) for January averaged between 1979 and 2003. January is on average the wettest month for all locations (http://iridl.ldeo.columbia.edu/). The coral sites are indicated as follows: SE, Seychelles; CH, Chagos; RE, Réunion; MA, Mayotte; IF, Ifaty.

2001; Hendy *et al*. 2002; Marshall & McCulloch 2002; Quinn & Sampson 2002). The oxygen isotope composition is the most widely used tool in coral palaeoclimatology. In regions with a constant hydrological balance, δ^{18}O provides SST variations, and in regions with variations in the evaporation–precipitation (EP) balance and/or oceanic advection, it provides variations in the isotopic composition of sea water ($\delta^{18}O_{\text{sea water}}$). Sr/Ca ratios have been shown to be the most robust thermometer in corals unaffected by sea-water variations (Alibert & McCulloch 1997; Gagan

et al. 1998; Marshall & McCulloch 2002; Quinn & Sampson 2002). Consequently, coupled measurements of coral Sr/Ca ratios and δ^{18}O therefore allow reconstruction of past changes in δ^{18}O of sea water by subtracting the thermal component of δ^{18}O based on the Sr/Ca-SST estimates (Corrège *et al*. 2000; Hendy *et al*. 2002; Ren *et al*. 2002). The effect of salinity can be resolved from the residual δ^{18}O signal $[\Delta\delta^{18}\mathrm{O} = \partial\delta^{18}\mathrm{O}/\partial T^{*}[T_{^{18}\mathrm{O}} - T_{\mathrm{Sr/Ca}}]]$ by using the relationship between salinity and $\delta^{18}\mathrm{O}_{\text{sea water}}$ inferred from observations and modelling studies (Schmidt 1999; Delaygue *et al*. 2001).

The importance of corals as a palaeoproxy is that their potentially long lifetime (100–400 years) and fast growth rate (1–2 cm yr^{-1}) provides high-resolution geochemical records for several centuries that allow study of natural climate variability under different boundary conditions, such as during the so-called Little Ice Age (1400–1850). In particular, fossil corals can provide insight into seasonality changes during the Holocene (last 10 kyr) or the Last Interglacial (125–131 kyr) (Gagan *et al*. 1998; Hughen *et al*. 1999; Corrège *et al*. 2000; Tudhope *et al*. 2001). Such information is key to understanding the processes that controlled past climate variations and hence predicting future climate change.

Recent coral records in the Indian Ocean show great potential for resolving the El Niño–Southern Oscillation (ENSO) and monsoon interaction as expressed in SST variations (Charles *et al*. 1997, 2003; Cole *et al*. 2000; Cobb *et al*. 2001; Zinke *et al*. 2004*a*, *b*) and precipitation anomalies (Pfeiffer *et al*. 2004*a*). In addition, oceanic variability (Tudhope *et al*. 1996; Kuhnert *et al*. 1999, 2000) and internal Indian Ocean phenomena, such as the tropical dipole mode, are manifested in several coral records (Marshall & McCulloch 2001; Abram *et al*. 2003). Instrumental records of climate variability from the Western Indian Ocean are generally scarce and short and thus do not fully delimit the extent to which ENSO or internal Indian Ocean phenomena modulate interannual and interdecadal SST variability. In contrast, high-resolution coral records dating back several centuries provide an excellent tool for the reconstruction of past surface ocean variability.

Here, we present a set of coral records from *Porites* sp. from the Western Indian Ocean covering the past 120–336 years. We show the results of oxygen isotope and trace element studies and their link to regional and global climatic patterns. The following questions will be addressed using coral δ^{18}O records from the Western Indian Ocean. Are the coral δ^{18}O records representative for regional climate variability, i.e. SST and/or precipitation? Does the EP balance changes through time, and if so, on what time-scales? Does coral δ^{18}O record variations in the South Equatorial Current (SEC) and Indonesian Throughflow? Is the zonal tropical Indian Ocean–ENSO teleconnection stable through time?

2. Regional setting of the coral sites

The climate of the Indian Ocean north of 10° S is dominated by the Asian monsoon system, which is characterized by a seasonal reversal of surface winds and a distinct seasonality in precipitation (Webster *et al*. 1998). The monsoon circulation is driven by the pressure gradients resulting from differential heating of land and ocean, modified by the rotation of the Earth. During boreal winter (NE monsoon), northeasterlies originating from the area of high surface pressure over the cold South Asian continent sweep over the Northern Indian Ocean. These airstreams meet the

Southern Hemisphere southeast trade winds in the Intertropical Convergence Zone (ITCZ). This zone is broadly embedded in a zone of high SSTs, and also features marked convergence and abundant precipitation. Very pronounced changes in temperature and airflow fields take place in April and May, marking the changeover to summer monsoon circulations. The circulation of the boreal summer monsoon is characterized by the highest surface temperatures over the South Asian continent and the adjacent sea areas. Maximum wind speeds occur in the Arabian Sea, the Bay of Bengal and in the core of the Southern Hemisphere trades. Evaporation is high in the regions of maximum wind intensity, and consequently the bulk of the moisture precipitated over southern Asia during the summer monsoon originates from the Southern Hemisphere (Hastenrath & Greischar 1993).

The strongest interannual signal in the Indian Ocean climate is the ENSO (Jury *et al*. 2002; Allan *et al*. 2003; Krishnamurthy & Kirtman 2003). The ENSO teleconnection pattern is modulated by interdecadal changes. Webster *et al*. (1998) distinguished three different regimes in ENSO-monsoon variability:

(i) before 1920, the two weather phenomena showed high variance and were tightly coupled;

(ii) from 1920 to 1960, there was little variability and correlations were zero; and

(iii) after 1960, there was high variance and higher correlations.

Kumar *et al*. (1999) reported that the historical relationship between the Asian monsoon and ENSO has broken down in recent decades, with reduced monsoon variability even when ENSO is strong.

The coral records assembled here were collected from tropical to subtropical regions within the Western Indian Ocean that are influenced by natural modes of oscillation in the Indian Ocean (monsoon) and also show strong interannual variability associated with the ENSO phenomenon (figure 1). The tropical sites include Seychelles, the Chagos Archipelago and Mayotte (Comoro Archipelago), and the subtropical sites include La Réunion and Ifaty (off Southwestern Madagascar).

The Chagos Archipelago lies in the central tropical Indian Ocean within a region with the highest total annual rainfall in the entire Indian Ocean (5° S, 73° E, figure 1*b*). Precipitation maxima at Chagos usually occur during the NE monsoon (December–February), when the Chagos is under the influence of the ITCZ. The isotopic composition of rainfall has been measured at Diego Garcia, an atoll in the south of the Chagos Archipelago. Measurements show that rainfall is depleted in δ^{18}O during the NE monsoon (International Atomic Energy Agency 1994). Chagos SSTs are relatively stable throughout the year, varying by less than 2 °C annually (Reynolds & Smith 1994). During warm ENSO events, precipitation significantly increases while SST typically increases by 0.5–1 °C (Reynolds & Smith 1994). The Chagos coral records were examined to see if coral δ^{18}O reflects rainfall variability, i.e. ITCZ variability and to establish the robustness of the ENSO winter monsoon rainfall teleconnection.

The climate of the granitic Seychelles (Mahé; 5° S, 55° E) is dominated by the seasonal reversal of the monsoon. During the boreal summer, the southwest monsoon season, Mahé experiences southwesterly trade winds. It is the cool and dry season of the year and evaporation is high. The trades are stronger on the eastern coast of the

island. This is due to the high relief of Mahé island (900 m) that produces an effective climatic barrier for lower tropospheric winds. During the boreal winter, the island is influenced by the ITCZ and most of the total annual rainfall falls during that season. Local climatic differences during this season are less pronounced. SSTs in Seychelles vary seasonally by *ca.* 3–4 °C (figure 1*a*). The Seychelles lie within a region where ENSO-induced SST anomalies exceed 0.5 °C (figure 2). The Mahé coral records were examined to determine whether they are a good proxy of SST variability on seasonal to decadal time-scales and whether they represent a good palaeo-monsoon proxy. We also determine whether the ENSO teleconnection has been stable through time.

Mayotte (13° S, 45° E) is situated within the Northern Mozambique Channel, and the climate is dominated by the seasonal reversal of the monsoon (figure 1). The NE monsoon season is very warm and humid, and evaporation is high. During the boreal summer, the southwesterly trades are less powerful due to the orographic effect of Madagascar. Mayotte also lies within a region of tropical cyclone activity. SSTs vary seasonally by 3–4 °C (figure 1*a*). ENSO-induced SST anomalies exceed 0.5 °C (figure 2). This study assesses whether or not changes in the EP balance influence coral δ^{18}O, and, if so, on what time-scales. The stability of the ENSO teleconnection at this site is compared with that of the Seychelles.

La Réunion (21° S, 55° E) is situated within the southern subtropical Indian Ocean and the climate is dominated by the year-round southeasterly trade winds. Evaporation exceeds precipitation in the annual mean. SST has an annual average variation of *ca.* 4 °C (figure 1*a*). Réunion lies within the path of the South Equatorial Current (SEC), which is the most powerful and persistent current in the Indian Ocean and carries the bulk of the waters from the Indonesian Throughflow (Gordon *et al.* 1997). Recent observations show substantial variability in the transport of Indonesian Throughflow waters during ENSO episodes (Meyers 1996; Godfrey 1996). In addition, historical salinity measurements show a strengthening of the SEC in the 1950–1975 interval compared with the present (Conkright *et al.* 2001). This paper examines the coral records to establish whether the EP balance or salinity in the Southwestern Indian Ocean change over time, and the relationship between coral δ^{18}O and ENSO. A fundamental question is the degree to which the coral δ^{18}O record indicates variations in the strength of the SEC and Indonesian Throughflow.

Ifaty reef (23° S, 43° E) lies off the southwestern coast of Madagascar in the path of the southward flow through the Mozambique Channel (figure 1). This flow is part of the warm surface flow of the global ocean circulation (DiMarco *et al.* 2002; de Ruijter *et al.* 2002, 2004; Schouten *et al.* 2002, 2003). The climate is dominated year round by the southeasterly trades and evaporation exceeds precipitation in the annual mean. Precipitation only reaches significant amounts during December–March (figure 1*b*), and is associated with the SE–NW orientated cloud bands stretching from the Western Indian Ocean towards South Africa (Todd & Washington 1999). SST varies seasonally by 6 °C (figure 1*a*; Reynolds & Smith 1994). ENSO is known to influence the EP balance over the Southwestern Indian Ocean and southern Africa (Tyson 1986; Reason & Mulenga 1999; Reason & Rouault 2002; Richard *et al.* 2000). This paper uses the coral record to determine whether the EP balance has changed through time and if so, whether it has been influenced by ENSO. Research questions focus on the stability of the ENSO teleconnection through time and the degree to which regional processes contribute to changes in the EP balance.

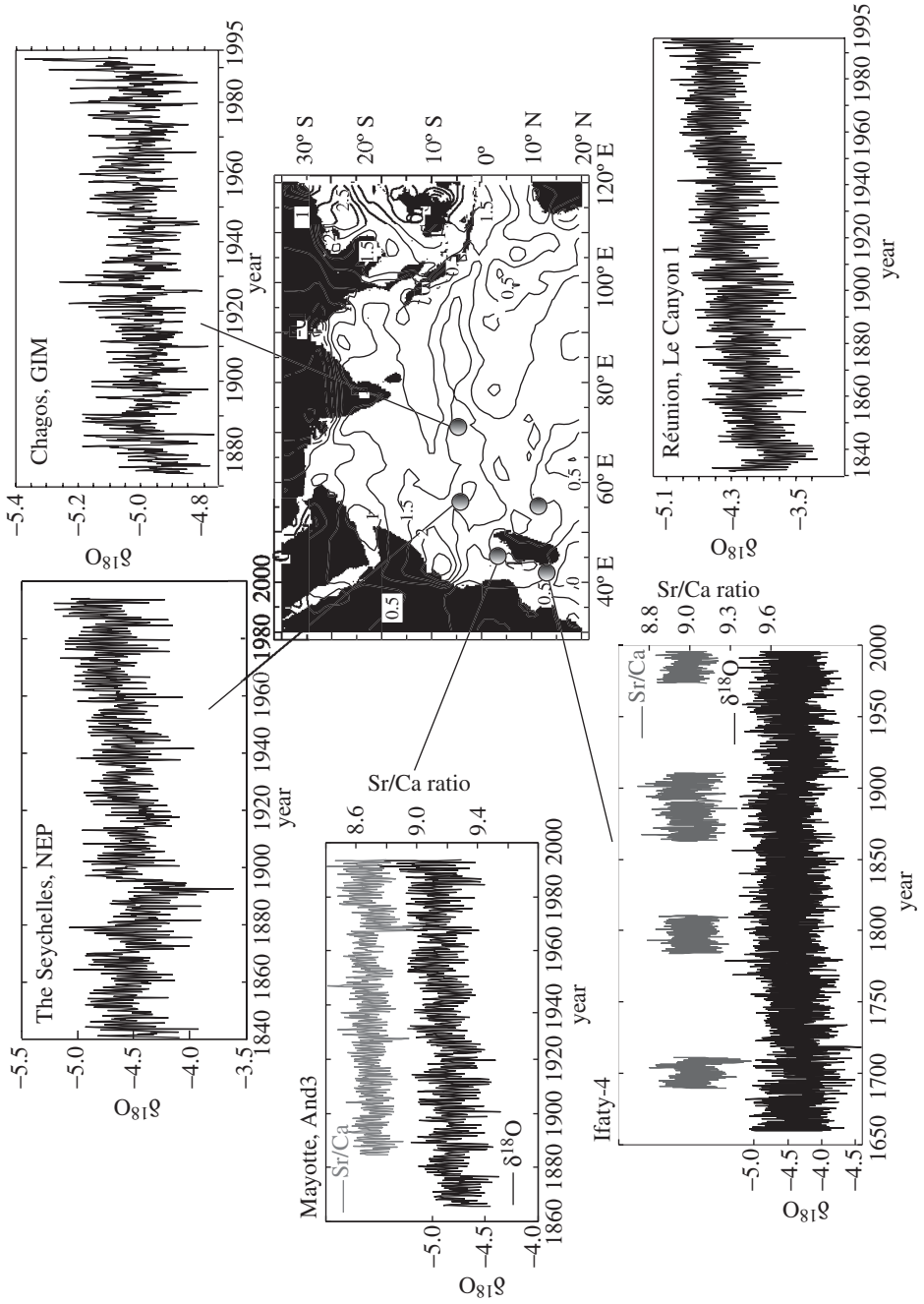

Figure 2. Map of coral core locations superimposed on the February 1998 SST anomaly field (from Reynolds *et al*. 2002) illustrating their sensitivity to SST anomalies during the strong ENSO of 1998 (http://iridl.ldeo.columbia.edu/). The sources for the coral data are as follows: Chagos, Réunion and Seychelles (Pfeiffer 2002; Pfeiffer *et al*. 2004*a–c*), Mayotte and Ifaty (Zinke *et al*. 2004*a*, *b*).

Table 1. *Location, coral genus, living depth, core length, mean growth rate, time-interval analysed and sampling resolution for all Western Indian Ocean corals studied for this article*
(A, living depths (m); B, core length (m); C, mean growth rate (mm yr^{-1}).)

location	coral species	A	B	C	time-interval analysed	sampling resolution
Chagos, GOI-5	*Porites lobata*	1.8	1.30	14±1	1962–1996	bimonthly
Chagos, GIM	*Porites solida*	3	2.35	14±1	1876–1996	bimonthly
Seychelles, NEP	*Porites solida*	9	2.03	11±1.5	1840–1994	bimonthly
Mayotte, And3	*Porites solida*	2	2.38	14±2	1865–1995	bimonthly
Réunion, Le Canyon 1	*Porites* sp.	12	1.95	9.5±1.5	1832–1995	bimonthly
Madagascar, Ifaty-4	*Porites lobata*	1.8	4.06	10±1.5	1659–1920	bimonthly
					1920–1995	monthly

3. Materials and methods

(*a*) *Sample collection and preparation*

The coral cores were drilled in the years 1994–1998 from massive colonies of the genus *Porites* sp. (*Porites lobata, Porites lutea, Porites solida)*, using a commercially available pneumatic drill (table 1). Cores of a length varying between 2 and 4 m with a diameter of 36 mm were drilled vertically along the growth axis. Cores were duplicated to ensure reproducibility. All cores were sectioned to a thickness of 5 mm and slabs were rinsed several times with demineralized water and dried with compressed air. To ensure complete removal of any moisture within the coral skeleton, individual samples were put into an oven for 24 h at 40 °C. The slabs were X-rayed to determine annual density banding and hence develop an initial chronology.

(*b*) *Sampling*

A high-resolution profile was drilled using a computer-controlled drilling device, along the growth axis as determined from X-radiograph-positive prints. Subsamples were drilled at a distance of 1 and 2 mm using a 0.5 mm dental drill at 1000 RPM. The drilling depth was 3 mm. The growth rate of the corals sampled averaged 9–16 mm yr^{-1} (table 1). Thus the 1 or 2 mm sample spacing provides approximately monthly or bimonthly resolution, respectively.

(*c*) *Chronology*

In order to compare the geochemical records recovered from coral samples with instrumental data, the record must be converted from the depth domain to the time domain. The density couplets in corals were used to establish an initial chronology. This preliminary age model was refined using the pronounced seasonal cycle in $\delta^{18}O$ and Sr/Ca to develop a chronology for the entire coral core. The seasonal maxima (minima) of $\delta^{18}O$ and Sr/Ca values were assigned to the coldest/driest (warmest/wettest) month at a given site based on long-term climatological data. At all the stations sampled, the exact timing of the coldest and warmest month varies by about 1–2 months between the years. This methodology thus creates a time-scale error of about 1–2 months in any given year. Based on the seasonal maxima and

minima the δ^{18}O and Sr/Ca time-series were interpolated linearly into 6 and 12 equidistant points for any given year using the Analyseries software (Paillard *et al.* 1996) to produce a monthly and a bimonthly time-series. Hence we generate time-series of coral δ^{18}O and Sr/Ca for different seasons of the year (January/February (JF), March/April (MA), May/June (MJ), July/August (JA), September/October (SO), November/December (ND)) over the entire record.

(*d*) *Analysis*

For δ^{18}O analysis the samples were reacted with 100% H_3PO_4 at 75 °C in an automated carbonate reaction device (Kiel Device) connected to a Finnigan MAT 252 mass spectrometer. Average precision based on duplicate sample analysis and on multiple analysis of NBS 19 is ±0.07‰ for δ^{18}O.

Sr/Ca ratios were measured at the same resolution as δ^{18}O samples with an inductively coupled plasma atomic emission spectrometer (ICP-AES), which simultaneously collected the respective elemental emission signals. Measurements were carried out at the Institute für Chemie und Biologie des Meeres at the University of Oldenburg following the technique reported by Schrag (1999). Instrumental precision was typically better than ±0.15% relative standard deviation (RSD) for Ca and ±0.08% RSD for Sr (2σ). For the Sr/Ca ratios the error was better than ±0.2% RSD (2σ). The reproducibility of the Sr/Ca ratios of replicate measurements performed on different days was ±0.3% RSD or 0.005 mmol mol^{-1} (2σ).

(*e*) *Advanced statistics*

The application of univariate and multivariate statistical techniques aims to identify regional and/or large-scale climate variability in coral proxy data. Because several studies have found a major shift in the interaction between climate variability in the Indian Ocean sector and ENSO (Trenberth 1990; Kumar *et al.* 1999; Kinter *et al.* 2002), the stationarity of the relationship between Indian Ocean coral proxies and ENSO is a crucial aspect in the interpretation of the proxy data. Therefore, statistical parameters (e.g. correlation coefficients or empirical orthogonal functions (EOFs)) are estimated from overlapping temporal sample domains. They allow a first guess of the temporal stability of the statistical parameters. Note that the choice of the sample size should be large enough to establish appropriate estimates of the statistical parameters. On the other hand, the temporal sample interval limits the accuracy of detecting instationarities.

EOF analysis was applied to the coral dataset. A 31-year data window was used to produce a running EOF analysis. The EOF analysis decomposes the covariance matrix of the corals into its eigenmodes, i.e. into the dominant patterns of spatio-temporal variability. Thus, the EOF provides insight into the large-scale climatic variability recorded in Indian Ocean corals. Since this work was focused on ENSO variability, the Palmyra coral record from the central Pacific Ocean, which is an excellent proxy for ENSO (Cobb *et al.* 2001), was included in the multi-proxy dataset. By inspecting the temporal stability of the leading EOF mode, it was possible to improve the climatic interpretation of the region by the study of a network of coral proxy data.

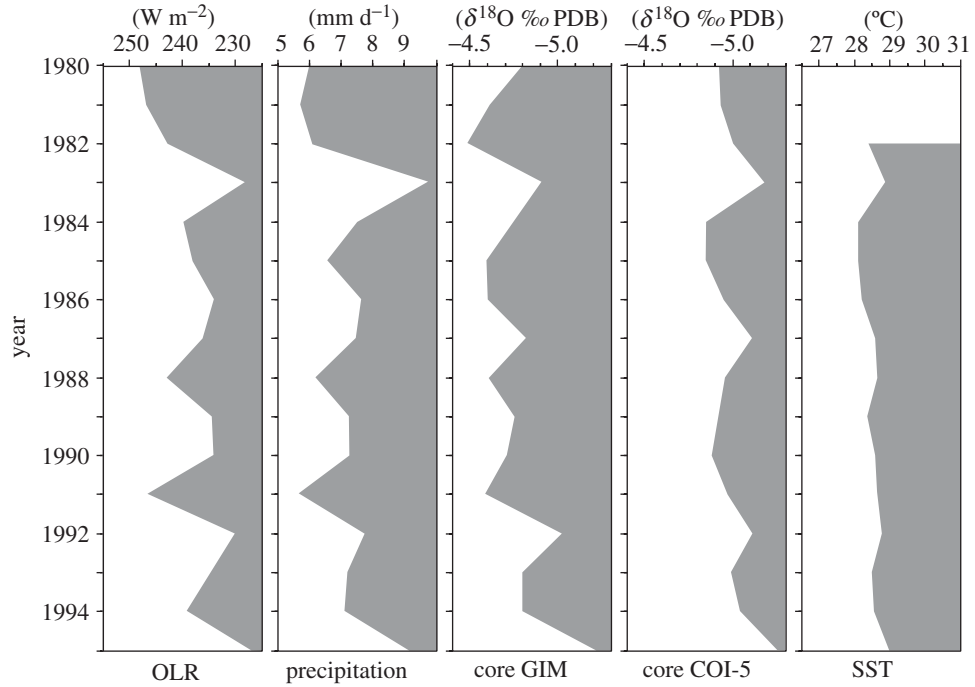

Figure 3. Mean December–March OLR, precipitation (Xie & Arkin 1996), coral δ^{18}O of core GIM and COI-5, SST from NCEP/NCAR (Reynolds & Smith 1994). Data from Pfeiffer *et al.* (2004*a*).

4. Results and discussion

(*a*) *Coral records*

Western Indian Ocean coral δ^{18}O records in general display a century-scale trend over the twentieth century (figure 2). This trend of decreasing δ^{18}O with time cannot be solely interpreted as reflecting SST changes, since changes in the EP balance and oceanic advection also influence the δ^{18}O of sea water. The seasonal amplitudes of each record are distinct and follow the local SST and EP patterns (Pfeiffer 2002; Pfeiffer *et al.* 2004*a–c*; Zinke *et al.* 2004*a*, *b*).

In the following section we will determine the relation of each of the coral δ^{18}O (and Sr/Ca, when available) time-series to local and regional climate variability. Hence we will resolve the interannual to interdecadal variability in the proxy records.

(*b*) *Chagos*

We have analysed the oxygen isotope composition of two cores from Peros Banhos atoll with bimonthly resolution (Pfeiffer 2002; Pfeiffer *et al.* 2004*a*). Core COI-5 is 34 years and core GIM is 124 years long. Over the period of overlap, the correlation coefficient between the annual mean δ^{18}O series of the two corals is 0.64 ($p < 0.001$). The corals precisely record the depletion in δ^{18}O sea water during the NE monsoon season by showing negative δ^{18}O anomalies (figure 3). There is a high correlation between mean December–March coral δ^{18}O, precipitation and outgoing long-wave

Table 2. *Correlation matrix between mean December–March OLR, precipitation (Xie & Arkin 1996), GIM coral δ^{18}O, COI-5 coral δ^{18}O, and NCEP-SST (Reynolds & Smith 1994)*

	OLR	precipitation	GIM	COI-5	SST
OLR	1				
precipitation	−0.89	1			
GIM	0.79	−0.78	1		
COI-5	0.58	−0.65	0.75	1	
SST	−0.41	0.44	−0.66	−0.82	1

radiation (OLR), but also between δ^{18}O and SST (table 2). The δ^{18}O and SST series in figure 3 are scaled according to the coral δ^{18}O/temperature relationship (0.2‰/1 °C) (Juillet-Leclerc & Schmidt 2001). Based on this relationship, the maximum SST contribution to mean summer coral δ^{18}O is only 29% (GIM) and 50% (COI-5). The SST record does not show as marked variations in the amplitude of the annual cycle as the coral δ^{18}O and rainfall records. Thus, coral δ^{18}O at this site can be used as a proxy of the temporal variability of precipitation patterns associated with the ITCZ through amplitude modulations of the annual cycle.

(*c*) *Seychelles*

A monthly resolved 150-year coral δ^{18}O record from Beau Vallon Bay (western coast of Mahé) was published by Charles *et al*. (1997) (4.3° S, 55° E). The seasonal and interannual coral δ^{18}O shows a high correlation to local and 1° × 1° gridded SST (Reynolds & Smith 1994) between 1982 and 1995 (Charles *et al*. 1997). Thus, it has been suggested that this record provides a tool for tropical SST reconstruction (Charles *et al*. 1997). Moreover, interannual variability was shown to be significantly coherent with Niño-3 SST, which captures the ENSO-related SST anomalies in the tropical Pacific. The Western Indian Ocean SST–ENSO relationship was shown to have been constant over the last 100 years (Charles *et al*. 1997).

A new *Porites* colony (NEP) was drilled on the eastern side of Mahé in 1995, which is more exposed to the southeast trades (4.3° S, 55° E). Over the period from 1946 to 1995, the NEP record shows a persistent linear correlation with Arabian Sea SST ($r = -0.63$, $p < 0.001$; figure 4*a*) (Pfeiffer 2002; Pfeiffer *et al*. 2004*b*). Spatial Correlation analysis (Pfeiffer *et al*. 2004*b*) reveals a strong relationship with Arabian Sea SST in the SW monsoon season, when the Arabian Sea cools due to wind-driven evaporation and coastal upwelling (Rao & Sivakumar 2000; Vinayachandran 2004).

In contrast, the coral record published by Charles *et al*. (1997) does show a weak relationship with Arabian Sea SST in the 1946–1995 period ($r = -0.43$, $p < 0.04$; figure 4*b*). In fact, the coral record diverges from local grid-SST (ERSST (Smith & Reynolds 2003); for 1946–1995, $r = -0.29$, $p < 0.04$) prior to the 1980s. These discrepancies may result from local climatic effects specific to the coral site, or biological factors that affect the incorporation of the stable isotopes into the coral skeleton (see, for example, McConnaughey 1989). The reliability of the Seychelles corals as monitors of regional and remote climatic processes clearly needs further investigation and a thorough analysis of both coral records.

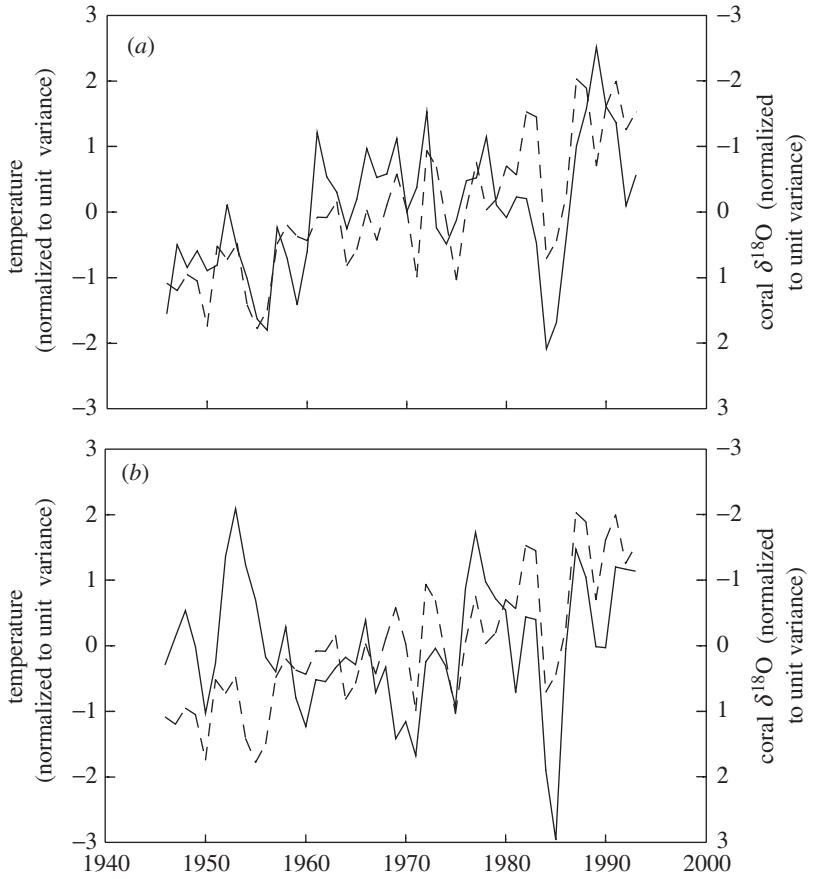

Figure 4. Relationship of coral δ^{18}O and Arabian Sea temperatures. Arabian Sea temperatures are averaged over 5° S to 20° N, and 50° E to 70° E (http://climexp.knmi.nl). The data are taken from the HadCRUT2 dataset, which combines land temperature anomalies with marine SST anomalies on a 5° × 5° grid-box basis (Parker *et al.* 1995). The Arabian Sea temperature series (dashed line) is plotted against (*a*) the new coral record taken from the east coast of Mahé (Pfeiffer *et al.* 2004*b*); (*b*) the coral from the west coast of Mahé, published by Charles *et al.* (1997). All indexes are normalized, and their correlations are shown in the panel. (*a*) $r = -0.63$, $p < 0.001$; (*b*) $r = -0.43$, $p < 0.04$.

(*d*) *Mayotte*

Core And-3 (12°39′ S, 45°06′ E) was drilled from a lagoonal reef within the north-eastern lagoon which has a maximum water depth of 40 m. The lagoon is flushed with oceanic waters via deep passages (greater than 30 m). A bimonthly resolved 135-year-long oxygen isotope record was generated (1865–1994) (figure 2). Additionally, Sr/Ca ratios were measured on bimonthly resolution back to 1884 to deconvolve the $\delta^{18}O_{\text{sea water}}$ component (figure 2). The correlation coefficient between bimonthly coral δ^{18}O and Sr/Ca ratios with lagoon SST is $r = -0.62$ and $r = -0.67$, respectively (figure 5). Occasionally, both coral δ^{18}O and Sr/Ca do not mirror annual mean SST variability accurately (figure 5). Mean annual Sr/Ca ratios show a correlation coefficient of $r = -0.46$ with lagoon SST for the period 1955–1994, whereas it is only

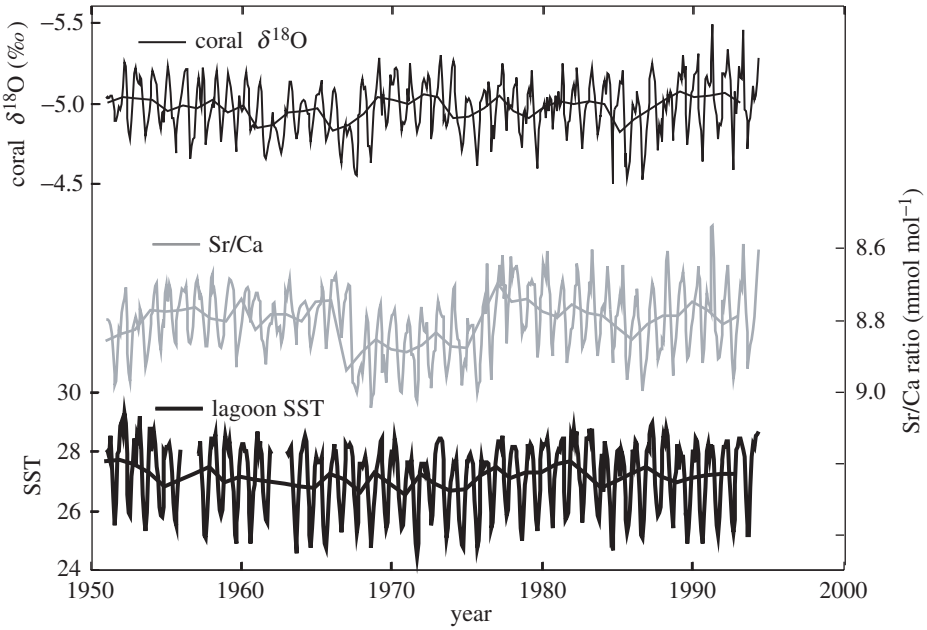

Figure 5. Bimonthly coral δ^{18}O time-series for core And-3 from Mayotte (thin solid line) (top). Sr/Ca ratios for core And-3 (greyish line) (middle). Monthly lagoon SST derived by regression of measured lagoon SST between 1999 and 2002 with observed air temperature (thick solid line) at Dzaoudzi weather station (Mayotte) for the same time-interval ($r^2 = 0.85$ (Nicet 2003)) (bottom). Annual mean values are superimposed on bimonthly values for each time-series. The correlation coefficient (top, $r = -0.62$; middle, $r = -0.67$) of each proxy time-series with lagoon SST is indicated for bimonthly resolution.

$r = -0.31$ for δ^{18}O. This might be due to slight environmental differences between lagoon and open ocean waters. By taking into account the SST values from Sr/Ca and SST observations, however, we reconstructed past $\delta^{18}O_{\text{sea water}}$ variability using the method of Ren *et al*. (2002) for the period of best data coverage (1951–1994) (not shown). First results indicate that similar variations in the $\delta^{18}O_{\text{sea water}}$ on decadal time-scales can be deduced by using either Sr/Ca-(SST) or lagoon SST (Zinke *et al*. 2004*a*). Thus, variations in the EP balance and salinity variations influence coral δ^{18}O. During the 1982/83 warm ENSO event, coral δ^{18}O indicates positive anomalies coincident with exceptionally high lagoon SST, most probably due to higher evaporation rates. Additionally, river run-off into the northern Mozambique Channel in response to rainfall variability during the NE monsoon season (December–March) may contribute to the coral δ^{18}O signal. Calibration of coral proxy signals with sea-water samples from the Mayotte lagoon was initiated in 2003 in order to thoroughly interpret environmental factors retrieved from corals. Once these data are generated, the Mayotte corals can potentially provide insights into the spatial and temporal variability of surface waters in the northern Mozambique Channel.

(*e*) *Réunion*

We have developed a 163-year bimonthly coral oxygen isotope record (Le Canyon-1; 21° S, 55° E (Pfeiffer 2004*c*)). On a seasonal scale, coral δ^{18}O reflects SST variations.

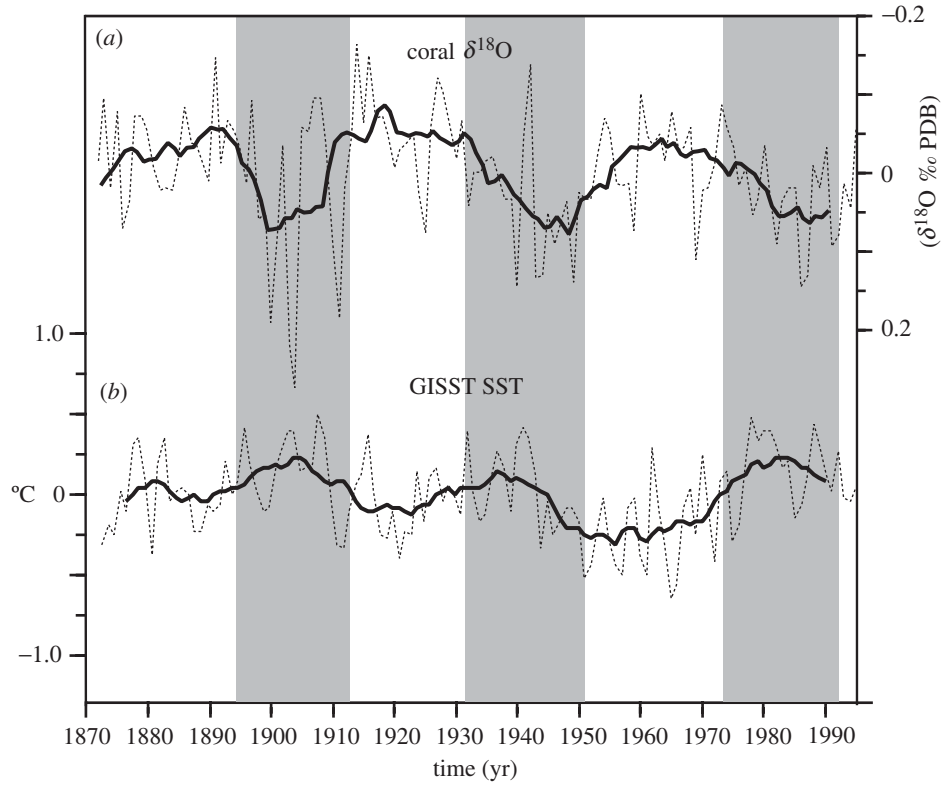

Figure 6. (*a*) Annual mean coral δ^{18}O (dashed line) and 11-point moving average (solid line) (Pfeiffer 2002; Pfeiffer *et al*. 2004*c*). (*b*) Annual mean SST from the GISST 2.3 dataset (dashed line) (Parker *et al*. 1995) and 11-point moving average (solid line). Coral δ^{18}O and SST are shown as anomalies relative to the mean for the period 1871–1995. The long-term trends have been removed.

Multidecadal variations in coral δ^{18}O are coherent with regional SST, but the sense of this relationship is of opposite sign to that expected from the coral δ^{18}O–temperature relationship (Pfeiffer *et al*. 2004*c*) (figure 6). This indicates multidecadal variations in surface salinity. The cause of the salinity variations may be linked to the wind-driven southern Indian Ocean gyre (Allan *et al*. 1995). Stronger surface winds lead to increased evaporation (and hence colder SST), but also to a strengthening of the SEC, which will advect low-salinity waters towards Réunion.

Interannual variability in the 6–7-year frequency band is the strongest signal in the coral record (Pfeiffer 2004*c*). The signal is coherent with the Southern Oscillation index (Allan *et al*. 1991), but not with the regional SST record. We suggest that the signal also results from variations in δ^{18}O sea water through changes in the strength of the SEC and/or the Indonesian Throughflow during ENSO (Meyers 1996; Godfrey 1996).

(*f*) *Ifaty*

A 336-year coral oxygen isotope record is reported from off Southwestern Madagascar (23° S, 43° E) with monthly (1920–1995) and bimonthly resolution (1659–1920)

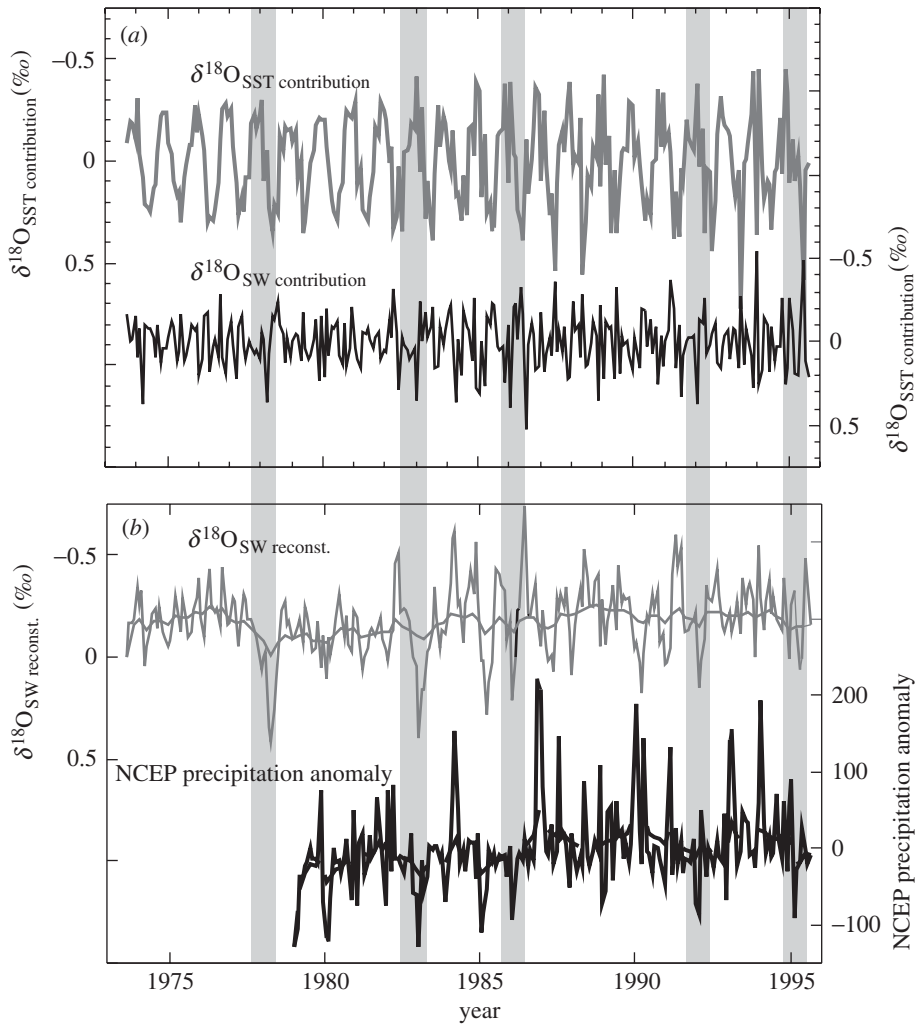

Figure 7. Demonstration of how the δ^{18}O sea-water component from coral δ^{18}O in the Ifaty coral was deconvolved following the method of Ren *et al.* (2002). This method separates SST and sea-water contributions in coral δ^{18}O by calculating the instantaneous changes in δ^{18}O and instrumental SST (or Sr/Ca). Thus, freshening or saltification of surface waters related to SST and atmospheric changes can be deduced. (*a*) Monthly variations in coral $\delta^{18}O_{SST\ contribution}$ versus coral $\delta^{18}O_{sea\text{-}water\ contribution}$ using SST from GISST 2.3 dataset (Rayner *et al.* 1996). (*b*) Reconstructed $\delta^{18}O_{\ sea\ water}$ variations using SST data from the GISST 2.3 dataset versus NCEP/NCAR precipitation anomaly (http://www.cdc.noaa.gov/cdc/data.ncep.reanalysis.derived.html). El Niño years are indicated by shaded vertical bars (http://www.cpc.noaa.gov:80/products/analysis_monitoring/ensostuff/ensoyears.html). Note the general association of positive $\delta^{18}O_{sea\ water}$ anomalies with deficient precipitation and also their occurrence during strong ENSO years (Zinke *et al.* 2004*b*).

(Zinke *et al.* 2004*a*, *b*) (figure 2). The coral oxygen isotope record primarily reflects SST variability on a seasonal scale (Zinke *et al.* 2004*b*). Sea-water oxygen isotope composition, calculated by subtracting the Sr/Ca derived temperature component,

contributes significantly to interannual variations in the coral isotope record (figure 7). During the mature phase of strong ENSO warm events (i.e. December 1982 to February 1983) regional evaporation off Southwestern Madagascar increases, which is shown by positive coral δ^{18}O anomalies (figure 7) (Zinke *et al.* 2004*b*). The Ifaty coral record is coherent with the Niño-3 index in the 2–4-year frequency band (Zinke *et al.* 2004*a*, *b*). Thus, our coral record is a tool for reconstructing the influence of ENSO induced large-scale atmospheric circulation anomalies on the EP balance in Southwestern Indian Ocean subtropical latitudes through the last 336 years (Zinke *et al.* 2004*c*).

(*g*) *Multi-proxy analysis*

The combination of several coral records spanning an ocean basin can be used for large-scale climate reconstructions (Evans *et al.* 1999). Therefore, one can focus on the variance that is common to all records in a certain frequency band, i.e. ENSO frequency. We performed running correlations and running EOFs to highlight the temporal correlation between each individual coral record and ENSO indices (figure 8). We used the Niño-3 index and the Palmyra coral δ^{18}O time-series as robust ENSO indices (Cobb *et al.* 2001). Thus, if we combine the Palmyra record with the Niño-3 index (Kaplan *et al.* 1998), the running EOF analysis should produce a stable EOF pattern. Adding potential ENSO signals measured in Indian Ocean corals, the EOF assigns a proper weight for each coral record. Figure 8 shows the results of the running EOF analysis. The first EOF is plotted against time (the coefficients of the first EOF are assigned to the centre year of the data window). The coefficients of Niño-3 and Palmyra coral are constantly high and have the opposite sign to that expected (SST higher, δ^{18}O lower) (figure 8*a*, *b*). The Seychelles coral record (Charles *et al.* 1997) has a constant coefficient of large magnitude (figure 8*a*, *b*). The coefficients of Chagos, Mayotte, Ifaty and La Réunion corals change their magnitude over the years (figure 8*a*, *b*). The Chagos coral joins the ENSO signal in the covariance structure only in the end of the twentieth century (figure 8*a*, *b*). We suggest that this may be the result from the amplification of the ENSO cycle, in conjunction with the observed eastward shift of the ENSO impacts from the Indian to the east Asian–Australian sector after 1970 (Kumar *et al.* 1999). This so-called 1970s shift weakens the Indian monsoon rainfall connection (Kumar *et al.* 1999), but it enhances the link between rainfall in the central Indian Ocean sector (i.e. austral summer) and ENSO (Pfeiffer *et al.* 2004*a*).

The variability in the La Réunion and Mayotte coral δ^{18}O in the early to mid twentieth century is related to the ENSO signal, but not in the late twentieth century (figure 8*a*, *b*). The correlation between Niño-3 SST and Ifaty shows a high correlation during phases when the ENSO forcing was strong, 1880–1920 and 1960–1995 (Webster *et al.* 1998; Zinke *et al.* 2004*b*). This is in good agreement with Richard *et al.* (2000), who showed that a strong teleconnection between Southwestern Indian Ocean SST (rainfall) and ENSO appears after 1970. Richard *et al.* (2000) concluded that the modified east–west circulation is partly forced by a warmer Southern Indian Ocean after 1970.

Interestingly, very similar results are obtained when the Niño-3 index is not included in the EOF analysis (figure 8*b*). Thus, the running EOF analysis might be able to detect non-stationary ENSO-proxy relationships in pre-industrial eras when the only source of climate information comes from proxy data.

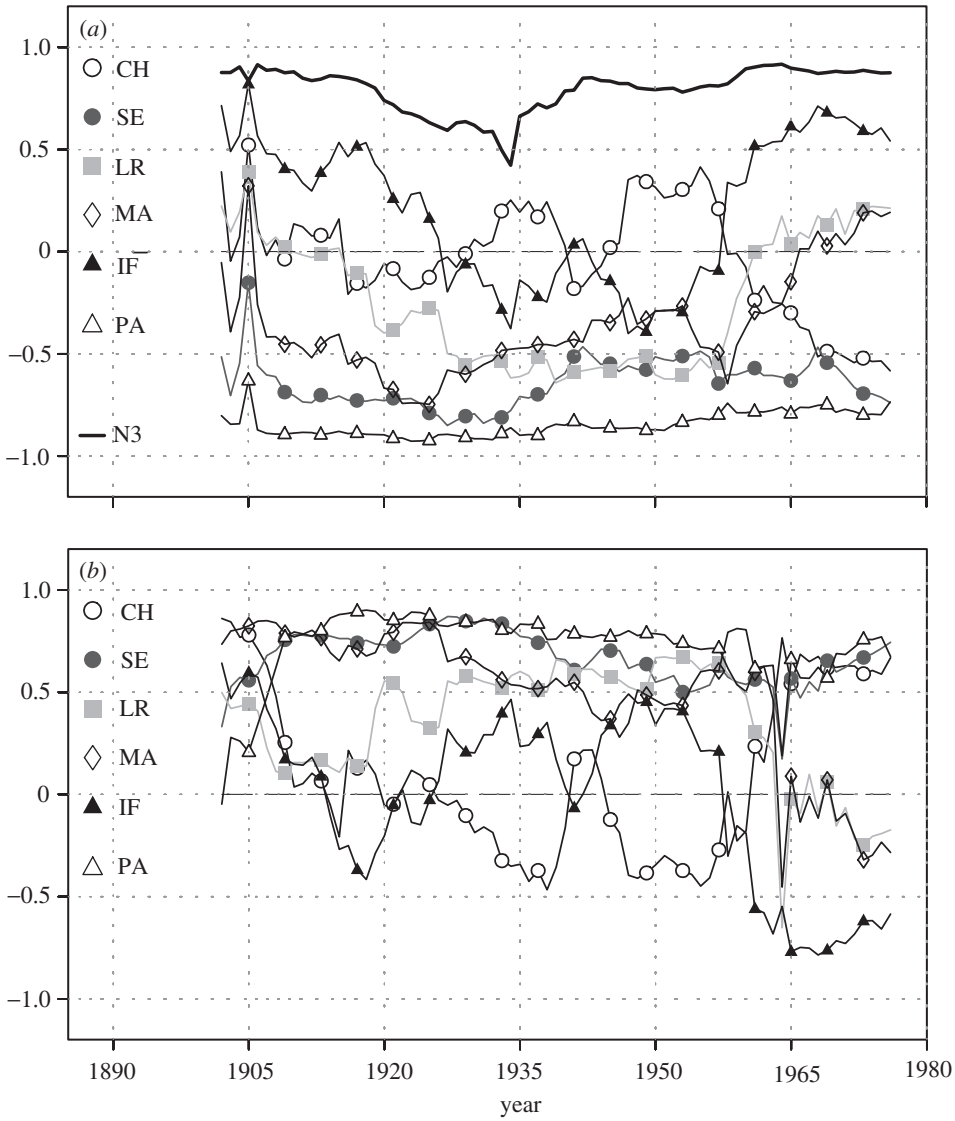

Figure 8. Running EOF analysis using a 31-year data window: (*a*) first EOF of the six-coral δ^{18}O time-series and the Niño-3 index; (*b*) first EOF when Niño-3 index is removed from the dataset. Note that the EOF analysis is applied to time-series of DJFM seasonal means over the years 1887–1991. Legend entries refers to corals from Chagos (CH) (Pfeiffer *et al*. 2004*a*), Seychelles (SE) (Charles *et al*. 1997), La Réunion (LR) (Pfeiffer *et al*. 2004*c*), Mayotte (MA), Ifaty (IF) (Zinke *et al*. 2004*a*, *b*), Palmyra (PA) (Cobb *et al*. 2001); N3 refers to the Niño-3 index (Kaplan *et al*. 1998).

The power of this analysis is further demonstrated by an example (figure 9). The multi-proxy data were altered in the following way. The Chagos coral was replaced by an artificial proxy. This artificial proxy was generated by summation of the normalized Niño-3 index $x(t)$ and normalized white noise $e(t)$. To simulate the non-stationary linear relationship a time-dependent linear regression coefficient

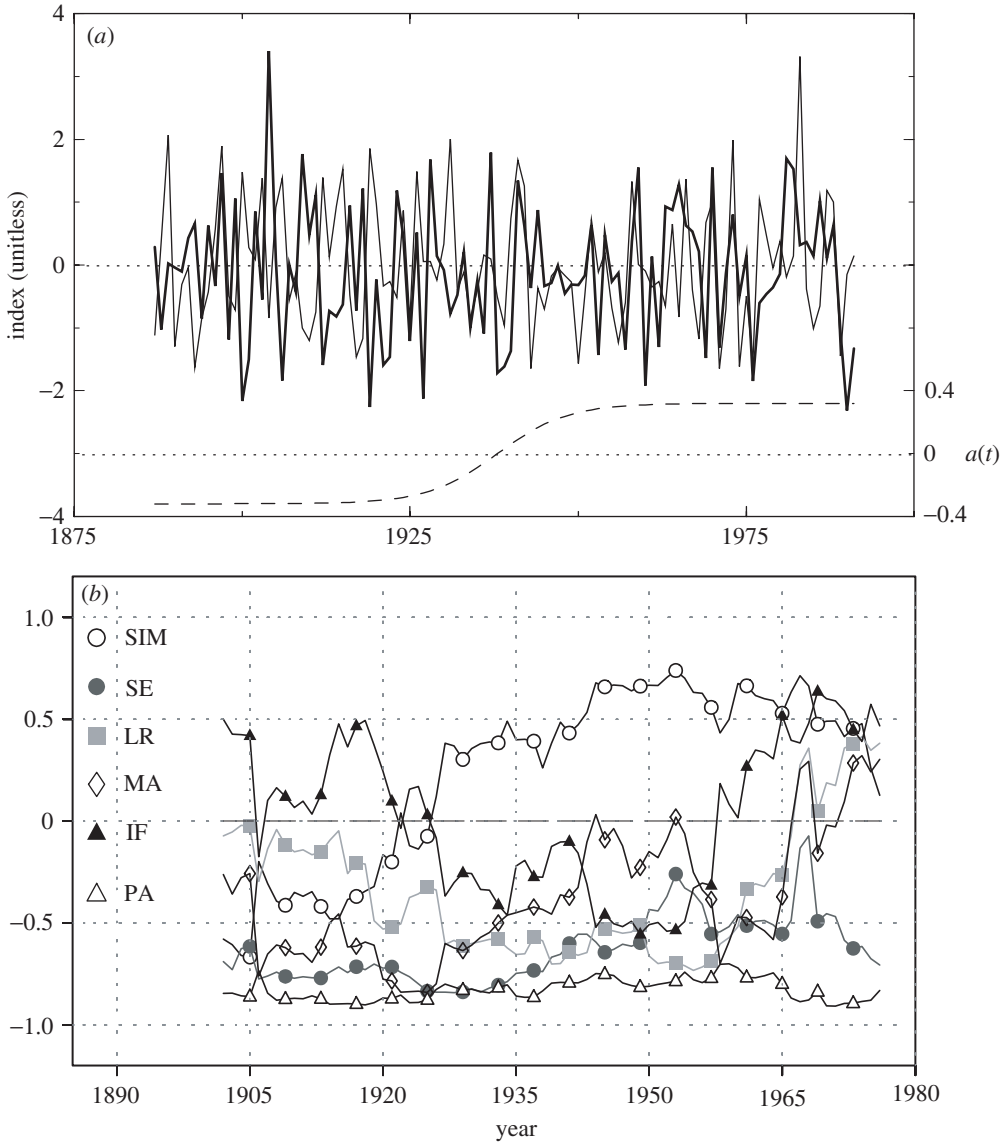

Figure 9. (*a*) Time-series of the simulated proxy time-series (thick grey line), the Niño-3 index (thin black line), and the linear regression coefficient between them (dashed line). (*b*) The running EOF analysis (using a 31-year window) as in figure 8*b*. Note that the artificial proxy (denoted as SIM) replaced the Chagos coral in the multivariate dataset.

$a(t)$ determined the signal-to-noise ratio. Thus, the artificial proxy was generated by the following equation:

$$y(t) = a(t)x(t) + \sqrt{1 - a(t)^2}e(t),$$

where

$$a(t) = 0.4\tanh[w(t - 1940)],$$

with $w = 10$ years, where t denotes the year (1887–1991).

In figure 9 the generated artificial proxy is shown together with the Niño-3 index. The shape of the regression coefficient $a(t)$ is also shown. Even though the correlation between this proxy and the Niño-3 index was rather low in this example, the running EOF analysis was able to identify the shift in the relationship. Another important result is the robustness of the EOF. Only small differences in the weight factors of the unchanged coral proxies were caused by the replacement of one proxy.

Even without appropriate statistical hypothesis tests, this technique provides a powerful tool for the multivariate proxy analysis. Of course, more work will be needed to identify the true power of this method.

5. Conclusions

This paper presents a network of coral oxygen isotope and/or Sr/Ca records covering the last 120–336 years spanning the western tropical to subtropical Indian Ocean. All records record regional climate variability. Chagos coral δ^{18}O records rainfall variability on interannual to interdecadal time-scales, the Seychelles coral δ^{18}O records interannual and decadal SST variations related to ENSO and the monsoon, Mayotte and Ifaty record changes in the hydrologic balance and Réunion records multidecadal variations in salinity propagated via changes in the strength of the South Equatorial Current.

The coral records show varying sensitivities to ENSO variability. The empirical orthogonal function analysis (EOF) using moving data windows is presented as a method to detect the ENSO-proxy relationship for each coral record. The Seychelles coral record shows a stationary relationship to ENSO; all other records show non-stationary ENSO-proxy relationships and/or higher sensitivity to ENSO induced large-scale circulation anomalies when the forcing is strong. Our results indicate that the coral δ^{18}O in combination with other proxies can be used to reconstruct temporal and spatial variations in the sea-surface temperature and the fresh water balance within the Indian Ocean on interannual to interdecadal time-scales. Such datasets will prove invaluable in attempts to successfully model past and predict future climate change.

We thank the TESTREEF-group (contract no. EV5V-CT 94-0447) for the drilling of the coral cores between 1994 and 1996 (CEREGE Aix-en-Provence, France; Université de Provence, Marseille, France; University of Glasgow, UK; Instituto per la Geologia Marina Bologna, Italy). H. Erlenkeuser (Leibniz Laboratory, University of Kiel) and M. Joachimski (University of Erlangen) kindly carried out the oxygen isotope analysis. We thank B. Schnetger (University of Oldenburg) for giving measurement capacity at the ICP-AES. This research was supported by the German Science Foundation (grant Du 129, 13-2 and 13-3) and by the German government through the KIHZ Initiative (grant BMBF 01LG9909). Comments by two anonymous reviewers helped improve the clarity of the manuscript. Work supported in part by the European Community's Human Potential Programme under contract HPRN-CT-2002-00221 (STOPFEN).

References

Abram, N. J., Gagan, M. K., McCulloch, M. T., Chappell, J. & Hantoro, W. S. 2003 Coral reef death during the 1997 Indian Ocean Dipole linked to Indonesian wildfires. *Science* **301**, 952–955.

Alibert, C. & McCulloch, M. T. 1997 Strontium/calcium ratios in modern Porites corals from the Great Barrier Reef as a proxy for sea surface temperature: calibration of the thermometer and monitoring of ENSO. *Paleoceanography* **12**(3), 345–363.

Allan, R. J., Nicholls, N., Jones, P. D. & Butterworth, I. J. 1991 A further extension of the Tahiti-Darwin SOI, early SOI results and Darwin pressure. *J. Clim.* **4**, 743–749.

Allan, R. J., Lindesay, J. A. & Reason, C. J. C. 1995 Multidecadal variability in the climate system over the Indian Ocean region during the austral summer. *J. Clim.* **8**, 1853–1873.

Allan, R. J., Reason, C. J. C., Lindesay, J. A. & Ansell, T. J. 2003 Protracted ENSO episodes and their impacts in the Indian Ocean region. *Deep-Sea Res. II* **50**, 2331–2347.

Charles, C. D., Hunter, D. E. & Fairbanks, R. G. 1997 Interaction between the ENSO and the Asian monsoon in a coral record of tropical climate. *Science* **277**, 925–928.

Charles, C. D., Cobb, K., Moore, M. D. & Fairbanks, R. G. 2003 Monsoon-tropical ocean interaction in a network of coral records spanning the 20th century. *Mar. Geol.* **201**, 207–222.

Cobb, K. M., Charles, C. D. & Hunter, D. E. 2001 A central tropical Pacific coral demonstrates Pacific, Indian, and Atlantic decadal climate connections. *Geophys. Res. Lett.* **28**(11), 2209–2212.

Cole, J. E., Fairbanks, R. G. & Shen, G. T. 1993 Recent variability in the Southern Oscillation: isotopic results from a Tawara Atoll record. *Science* **260**, 1790–1793.

Cole, J. E., Dunbar, R. B., McClanahan, T. R. & Muthiga, N. A. 2000 Tropical Pacific forcing of decadal SST variability in the Western Indian Ocean over the past two centuries. *Science* **287**, 617–619.

Conkright, M. E., Locarnini, R. A., Garcia, H. E., O'Brien, T. D., Boyer, T. P., Stephens, C. & Antonov, J. I. 2001 World Ocean Atlas 2001: objective analysis, data statistics, and figures. National Oceanographic Data Center Internal Report, vol. 17.

Corrège, T., Delcroix, T., Récy, J., Beck, W., Cabioch, G. & Cornec, F. L. 2000 Evidence for stronger El Niño–Southern Oscillation (ENSO) events in a mid-Holocene massive coral. *Paleoceanography* **15**(4), 465–470.

Delaygue, G., Bard, E., Rollion, C., Jouzel, J., Stiévenard, M., Duplessy, J.-C. & Ganssen, G. 2001 Oxygen isotope/salinity relationships in the northern Indian Ocean. *J. Geophys. Res.* C **106**(3), 4565–4574.

De Ruijter, W. P. M., Ridderinkhof, H., Lutjeharms, J. R. E., Schouten, M. W. & Veth, C. 2002 Observations of the flow in the Mozambique Channel. *Geophys. Res. Lett.* **29**(10), 140–142.

De Ruijter, W. P. M., van Aken, H. M., Beier, E. J., Lutjeharms, J. R. E., Matano, R. P. & Schouten, M. W. 2004 Eddies and dipoles around South Madagascar: formation, pathways and large-scale impact. *Deep-Sea Res. I* **51**, 383–400.

DiMarco, S. F., Chapman Jr, P., W. D. N., Hacker, P., Donohue, K., Luther, M., Johnson, G. C. & Toole, J. 2002 Volume transport and property distributions of the Mozambique Channel. *Deep-Sea Res. II* **49**, 1481–1511.

Druffel, E. R. M. & Griffin, S. 1993 Large variations of surface ocean radiocarbon: evidence of circulation changes in the southwestern Pacific. *J. Geophys. Res.* C **98**(11), 20 249–20 259.

Dunbar, R. B., Wellington, G. M., Colgan, M. W. & Glynn, P. W. 1994 Eastern Pacific sea surface temperatures since 1600 A.D.: the δ^{18}O record of climate variability in Galàpagos corals. *Paleoceanography* **9**(2), 291–315.

Evans, M. N., Fairbanks, R. G. & Rubenstone, J. L. 1999 The thermal oceanographic signal of El Niño reconstructed from a Kiritimati Island coral. *J. Geophys. Res.* C **104**(6), 13 409–13 421.

Gagan, M. K., Ayliffe, L. K., Hopley, D., Cali, J. A., Mortimer, G. E., Chappell, J., McCulloch, M. T. & Head, M. J. 1998 Temperature and surface-ocean water balance of the mid-Holocene tropical western Pacific. *Science* **279**, 1014–1018.

Godfrey, J. S. 1996 The effect of the Indonesian Throughflow on ocean circulation and heat exchange with the atmosphere: a review. *J. Geophys. Res.* C **101**(5), 12 217–12 237.

Gordon, A. L., Ma, S., Olson, D. B., Hacker, P., Field, A., Talley, L. D., Wilson, D. & Baringer, M. 1997 Advection and diffusion of Indonesian Throughflow water within the Indian Ocean South Equatorial Current. *Geophys. Res. Lett.* **24**(21), 2573–2576.

Hastenrath, S. & Greischar, L. 1993 The monsoonal heat budget of the hydrosphere–atmosphere system in the Indian Ocean sector. *J. Geophys. Res.* C **98**(4), 6869–6881.

Hendy, E. J., Gagan, M. K., Alibert, C. A., McCulloch, M. T., Lough, J. M. & Isdale, P. J. 2002 Abrupt decrease in tropical Pacific sea surface salinity at end of Little Ice Age. *Science* **295**, 1511–1514.

Hughen, K. A., Schrag, D. P., Jacobsen, S. B. & Hantoro, W. 1999 El Niño during the last interglacial period recorded by a fossil coral from Indonesia. *Geophys. Res. Lett.* **26**(20), 3129–3132.

International Atomic Energy Agency 1994 Environmental Isotope Data no. 10: World survey of isotope concentration in precipitation (1988–1991). Vienna: IAEA.

Juillet-Leclerc, A. & Schmidt, G. 2001 A calibration of the oxygen isotope paleothermometer of coral aragonite from *Porites*. *Geophys. Res. Lett.* **28**(21), 4135–4138.

Jury, M. R., Enfield, D. B. & Mélice, J.-L. 2002 Tropical monsoons around Africa: stability of El Niño–Southern Oscillation associations and links with continental climate. *J. Geophys. Res.* C **107**(10), 3151.

Kaplan, A., Cane, M., Kushnir, Y., Clement, A., Blumenthal, M. & Rajagopalan, B. 1998 Analysis of global sea surface temperature 1856–1991. *J. Geophys. Res.* **103**, 18 567–18 589.

Kinter, J. L., Miyakoda, K. & Yang, S. 2002 Recent change in the connection from Asian Monsoon to ENSO. *J. Clim.* **15**, 1203–1215.

Krishnamurthy, V. & Kirtman, B. P. 2003 Variability of the Indian Ocean: relation to monsoon and ENSO. *Q. J. R. Meteorol. Soc.* **129**, 1623–1646.

Kuhnert, H., Pätzold, J., Hatcher, B., Wyrwoll, K.-H., Eisenhauer, A., Collins, L. B., Zhu, Z. R. & Wefer, G. 1999 A 200-year coral stable oxygen isotope record from a high-latitude reef off Western Australia. *Coral Reefs* **18**, 1–12.

Kuhnert, H., Pätzold, J., Wyrwoll, K.-H. & Wefer, G. 2000 Monitoring climate variability over the past 116 years in coral oxygen isotopes from Ningaloo Reef, Western Australia. *Int. J. Earth Sci.* **88**, 725–732.

Kumar, K. K., Rajagopalan, B. & Cane, M. A. 1999 On the weakening relationship between the Indian monsoon and ENSO. *Science* **284**, 2156–2159.

Le Bec, N., Juillet-Leclerc, A., Corrège, T., Blamart, D. & Delcroix, T. 2000 A coral δ^{18}O record of ENSO driven sea surface salinity variability in Fiji (south-western tropical Pacific). *Geophys. Res. Lett.* **27**(23), 3897–3900.

Linsley, B. K., Wellington, G. M. & Schrag, D. P. 2000 Decadal sea surface temperature variability in the subtropical South Pacific from 1726 to 1997 A.D. *Science* **290**, 1145–1148.

McConnaughey, T. 1989 ^{1}3C and ^{1}8O isotopic disequilibrium in biological carbonates. I. Patterns. *Geochim. Cosmochim. Acta* **53**, 151–162.

McCulloch, M. T., Gagan, M. K., Mortimer, G. E., Chivas, A. R. & Isdale, P. J. 1994 A high-resolution Sr/Ca and δ^{18}O coral record from the Great Barrier Reef, Australia, and the 1982–1983 El Niño. *Geochim. Cosmochim. Acta* **58**(12), 2747–2754.

Marshall, J. F. & McCulloch, M. T. 2001 Evidence of El Niño and the Indian Ocean Dipole from Sr/Ca derived SSTs for modern corals at Christmas Island, Eastern Indian Ocean. *Geophys. Res. Lett.* **28**(18), 3453–3456.

Marshall, J. F. & McCulloch, M. T. 2002 An assessment of the Sr/Ca ratio in shallow water hermatypic corals as a proxy for sea surface temperature. *Geochim. Cosmochim. Acta* **66**(18), 3263–3280.

Meyers, G. 1996 Variations of Indonesian Throughflow and the El Niño–Southern Oscillation. *J. Geophys. Res.* C **101**(5), 12 255–12 263.

Nicet, J.-B. 2003 Mayotte lagoon temperature (1999–2002) and bleaching coral event. Report Collectivité départementale de Mayotte, Direction de l'Agriculture et de la Forêt, Service de Pêches et de l'Environnement Marin.

Paillard, D., Labeyrie, L. & Yiou, P. 1996 Macintosh program performs time-series analysis. *Eos* **77**, 379.

Parker, D. E., Folland, C. K. & Jackson, M. 1995 Marine surface temperature: observed variations and data requirements. *Clim. Change* **31**, 559–600.

Pfeiffer, M. 2002 Spatial and temporal variations in the hydrological balance recorded in Porites corals from the Western and Central Indian Ocean. PhD thesis, Christian-Albrechts-Universität zu Kiel.

Pfeiffer, M., Dullo, W.-C. & Eisenhauer, A. 2004*a* Variability of the Intertropical Convergence Zone recorded in coral isotopic records from the central Indian Ocean (Chagos Archipelago). *Quat. Res.* **61**, 245–255.

Pfeiffer, M., Dullo, W.-Chr. & Timm, O. 2004*b* Arabian Sea sea surface temperatures (SST) recorded by a Seychelles coral. Conference Poster, Discussion Meeting on Atmosphere–ocean–ecology dynamics in the Western Indian Ocean, The Royal Society, London, UK.

Pfeiffer, M., Timm, O., Dullo, W.-Chr. & Podlech, S. 2004*c* Oceanic forcing of interannual and multidecadal climate variability in the southern Indian Ocean: evidence from a 160 year coral isotopic record (La Réunion, 55° E, 21° S). *Paleoceanography* **19**, PA4006. (doi:10.1029/2003PA000964.)

Quinn, T. M. & Sampson, D. E. 2002 A multiproxy approach to reconstructing sea surface conditions using coral skeleton geochemistry. *Paleoceanography* **17**(4), 1062.

Quinn, T. M., Crowley, T. J., Taylor, F. W., Henin, C., Joannot, P. & Join, Y. 1998 A multicentury isotopic record from a New Caledonia coral: interannual and decadal sea surface temperature variability in the southwest Pacific since 1657 A.D. *Paleoceanography* **13**(4), 412–426.

Rao, R. P. & Sivakumar, R. 2000 Seasonal variability of near-surface thermal structure and heat budget of the mixed layer of the tropical Indian Ocean from a new global ocean temperature climatology. *J. Geophys. Res.* C **105**(1), 995–1015.

Rayner, N. A., Horton, E. B., Parker, D. E., Folland, C. K. & Hackett, R. B. 1996 Version 2.2 of the global sea-ice and sea surface temperature dataset. Climate Research Technical Note, Hadley Centre for Climate Prediction and Research, vol. 74, pp. 1–21.

Reason, C. J. C. & Mulenga, H. 1999 Relationships between South African rainfall and SST anomalies in the southwest Indian Ocean. *Int. J. Climatol.* **19**, 1651–1673.

Reason, C. J. C. & Rouault, M. 2002 ENSO-like decadal variability and South African rainfall. *Geophys. Res. Lett.* **29**, 10.1029.

Ren, L., Linsley, B. K., Wellington, G. M., Schrag, D. P. & Hoegh-Guldberg, O. 2002 Deconvolving the δ^{18}O seawater component from subseasonal coral δ^{18}O and Sr/Ca at Rarotonga in the southwestern subtropical Pacific for the period 1726 to 1997. *Geochim. Cosmochim. Acta* **67**(9), 1609–1621.

Reynolds, R. W. & Smith, T. M. 1994 Improved global sea surface temperature analysis. *J. Clim.* **7**, 929–948.

Reynolds, R. W., Rayner, N. A., Smith, T. M., Stokes, D. C. & Wang, W. Q. 2002 An improved *in situ* and satellite SST analysis for climate. *J. Clim.* **15**, 1609–1625.

Richard, Y., Trzaska, S., Roucou, P. & Rouault, M. 2000 Modification of the southern African rainfall variability/ENSO relationship since the late 1960's. *Clim. Dyn.* **16**, 883–895.

Schmidt, G. A. 1999 Oxygen-18 variations in a global ocean model. *Geophys. Res. Lett.* **25**(8), 1201–1204.

Schouten, M. W., de Ruijter, W. P. M., van Leeuwen, P. J. & Dijkstra, H. A. 2002 An oceanic teleconnection between the equatorial and southern Indian Ocean. *Geophys. Res. Lett.* **29**(16), 59–62.

Schouten, M. W., de Ruijter, W. P. M., van Leeuwen, P.-J. & Ridderinkhof, H. 2003 Eddies and variability in the Mozambique Channel. *Deep-Sea Res. II* **50**, 1987–2003.

Schrag, D. 1999 Rapid analysis of high-precision Sr/Ca ratios in corals and other marine carbonates. *Paleoceanography* **14**(2), 97–102.

Smith, T. M. & Reynolds, R. W. 2003 Extended reconstruction of global sea surface temperatures based on COADS data (1854–1997). *J. Clim.* **16**, 1495–1510.

Todd, M. & Washington, R. 1999 Circulation anomalies associated with tropical-temperate troughs in southern Africa and the south west Indian Ocean. *Clim. Dyn.* **15**, 937–951.

Trenberth, K. E. 1990 Recent observed interdecadal climate changes in the Northern Hemisphere. *Bull. Am. Meteorol. Soc.* **71**(7), 988–993.

Tudhope, A. W., Lea, D. W., Shimmield, G. B., Chilcott, C. P. & Head, S. 1996 Monsoon climate and Arabian Sea coastal upwelling recorded in massive corals from Southern Oman. *Paleobios* **11**, 347–361.

Tudhope, A. W., Chilcott, C. P., McCulloch, M. T., Cook, E. R., Chappell, J., Ellam, R. M., Lea, D. W., Lough, J. M. & Shimmield, G. B. 2001 Variability in the El Niño–Southern Oscillation through a glacial–interglacial cycle. *Science* **291**, 1511–1517.

Tyson, P. D. 1986 *Climate change and variability in Southern Africa*. Oxford University Press.

Vinayachandran, P. N. 2004 Summer cooling of the Arabian Sea during contrasting monsoons. *Geophys. Res. Lett.* **31**, L13306.

Webster, P. J., Magana, V. O., Palmer, T. N., Shukla, J., Tomas, R. A., Yanai, M. & Yasunari, T. 1998 Monsoons: processes, predictability, and the prospects for prediction. *J. Geophys. Res.* C **103**(7), 14 451–14 510.

Xie, P. & Arkin, P. 1996 Analysis of global monthly precipitation using gauge observations, satellite estimates, and numerical model predictions. *J. Clim.* **9**, 840–885.

Zinke, J. and the KIHZ Consortium 2004*a* Evidence for the climate during the Late Maunder Minimum from proxy data and model simulations available within KIHZ. In *The climate in historical times—towards a synthesis of Holocene proxy data and climate models* (ed. H. von Storch, E. Raschke & G. Floeser), pp. 397–414. Springer.

Zinke, J., Dullo, W.-C., Heiss, G. A. & Eisenhauer, A. 2004*b* ENSO and Indian Ocean subtropical dipole variability is recorded in a coral record off southwest Madagascar for the period 1659–1995. *Earth Planet. Sci. Lett.* **228**, 177–197.